Short Title: Metabolic modelling of CAM evolution

Article Title: Metabolic modelling of CAM cycling, CAM idling and the C_3-CAM continuum

Ignacius Tay Y. Y.[1], Kristoforus Bryant Odang[1] and C. Y. Maurice Cheung*[1]

[1]Yale-NUS College, 16 College Avenue West, Singapore 138527

*Corresponding author: C. Y. Maurice Cheung

Telephone: +65 66015276

Email: maurice.cheung@yale-nus.edu.sg

Funding information: Yale-NUS College (WBS R-607-265-233-121)

[1] **Author Contribution**

ITYY and CYMC conceptualised the modeling work. ITYY, KBO and CYMC carried out the model simulations. ITYY and CYMC co-wrote the manuscript. All authors read and approved the final manuscript.

One sentence summary:

Metabolic modelling of CAM cycling, CAM idling and the C_3-CAM continuum revealed the establishment of a starch-malate cycle in CAM evolution.

Abstract

The evolution of Crassulacean acid metabolism (CAM) is thought to be along a C_3-CAM continuum including multiple variations of CAM such as CAM cycling and CAM idling. Here, we applied large-scale constraint-based modelling to investigate the metabolism and energetics of plants operating in C_3, CAM, CAM cycling and CAM idling. Our modelling results suggested that CAM cycling and CAM idling could be potential evolutionary intermediates in CAM evolution by establishing a starch-malate cycle. Our model analysis showed that by varying the day-time stomatal conductance, there exists a C_3-CAM continuum with gradual metabolic changes, supporting the notion that evolution of CAM from C_3 could occur solely through incremental changes in metabolic fluxes. Along the C_3-CAM continuum, our model predicted changes in metabolic fluxes not only through the starch-malate cycle that is involved in CAM photosynthesis but also other metabolic processes including the mitochondrial electron transport chain and the tricarboxylate acid cycle at night. These predictions could guide engineering efforts in introducing CAM into C_3 crops for improved water use efficiency.

Keywords

CAM cycling, CAM evolution, CAM idling, Crassulacean acid metabolism, metabolic modelling, flux balance analysis

Introduction

Crassulacean acid metabolism (CAM) photosynthesis is an evolutionary descendant of C_3 photosynthesis, which is known to have evolved independently multiple times in at least 35 plant families comprising about 6% of flowering plant species (Winter and Smith, 1996; Silvera et al., 2010). CAM photosynthesis is typically associated with plants living in water-stressed conditions. By closing their stomata during the day and fixing carbon dioxide (CO_2) exclusively at night, CAM photosynthesis allows plants to use water more efficiently while fixing carbon for growth. The engineering CAM photosynthesis into C_3 crops has been suggested as a possible strategy to meet the demands on agriculture for food, feed, fibre, and fuels with the decreasing arable land area due to climate change (Borland et al., 2014). However, as a carbon-concentrating mechanism, CAM is thought to be more metabolically expensive than C_3, which suggests that transferring CAM pathways into C_3 plants would incur a crop yield penalty. To investigate the energetics of C_3 and CAM, large-scale metabolic models were applied which showed that engineering CAM into C_3 plants does not impose a significant energetic penalty given the reduction in photorespiration from the carbon-concentrating mechanism (Cheung et al., 2014; Shameer et al., 2018).

Besides the phylogenetic and ecological diversity of CAM plants, there is remarkable plasticity in its metabolism with multiple defined variations of CAM such as CAM cycling and CAM idling (Ting, 1985; Cushman, 2001). Silvera et al. (2010) generalised the idea of plasticity in CAM into a continuum of CAM evolution with differences in the degree for nocturnal and daytime net CO_2 uptake. Bräutigam et al. (2017) took the idea further to include C_3 as part of the C_3-CAM continuum and suggested that the evolution of C_3 to CAM only required incremental increases in metabolic fluxes. In this study, large-scale metabolic modelling was applied to investigate how CAM cycling and CAM idling fit into the continuum of CAM evolution and to identify to the changes in metabolic fluxes along the C_3-CAM continuum. The results from our modelling study could inform us about the energetics and metabolic alterations from C_3 to CAM, which could guide engineering efforts in introducing CAM into C_3 plants.

Results

Predicted metabolic fluxes of C_3, CAM, CAM cycling and CAM idling

In this study, we simulated the metabolism of leaves undergoing C_3, CAM, CAM cycling and CAM idling using a recently published core metabolic model of Arabidopsis which was used to model C_3 and CAM plants (Shameer et al., 2018). Minor modifications of the model were outlined in the Materials and Methods section. The constraints for simulating the core metabolic functions of mature leaves, namely export of sucrose and amino acids into the phloem and cellular maintenance, were set based on the values in Shameer et al. (2018). All simulations, except CAM idling, were constrained to have a phloem export rate of 0.259 μmol m^{-2} s^{-1} based on the value of C_3 plants in Shameer et al. (2018). The sets of constraints for modelling the four different modes of photosynthesis were summarised in Table 1. The primary objective function of minimising photon demand was used throughout this study, which allows us to study the metabolic efficiencies of the different modes of photosynthesis.

The model predictions of C_3 and CAM were very similar to that in Shameer et al. (2018) given the similarities in the constraints used. Carbon is fixed during the day in the C_3 flux prediction, whereas carbon is fixed at night in CAM with phospho*enol*pyruvate carboxykinase (PEPCK) being the main predicted route for malate decarboxylation. The core set of metabolic fluxes is depicted in Figure 1.

CAM cycling

Similar to C_3 plants, CAM cycling fixes carbon in the day. CAM cycling is characterised by its closed stomata at night with refixation of respiratory CO_2 and a small diel organic acid flux (Sipes and Ting, 1985; Cushman, 2001). To model CAM cycling, we applied the C_3 constraints with an additional constraint of setting CO_2 and O_2 exchange at night to zero to simulate the closure of the stomata. This resulted in a flux distribution that resemble a weak version of CAM with nocturnal malate accumulation and increase daytime starch accumulation. Phospho*enol*pyruvate carboxylase (PEPC) was predicted to be active only at night in CAM cycling for CO_2 refixation, in contrast to C_3 where PEPC was only active during the day. Another major difference between CAM cycling and C_3 is malate accumulation. While C_3 was predicted to have a very small amount of malate accumulates during the day, CAM cycling was predicted to have substantial amount of nocturnal malate accumulation (~20% of the amount of malate accumulation in CAM), which is consistent with what is known about CAM cycling. The nocturnal malate accumulation and CO_2

refixation via PEPC in CAM cycling were accompanied by changes in fluxes in other parts of metabolism. There was a larger flux through gluconeogenesis to convert malate into starch in the day, which led to more starch accumulation during the day in CAM cycling compared to C_3. For the decarboxylation of malate during the day, PEPCK and malic enzyme in the cytosol were predicted to be active in CAM cycling but not in C_3.

Given that CAM cycling has a higher daytime starch accumulation, it was predicted that CAM cycling has a larger glycolytic flux to convert starch into phospho*enol*pyruvate (PEP) for CO_2 refixation compared to C_3. The activities of most of the other reactions at night were similar in CAM cycling and in C_3 with CAM cycling having a slightly higher flux through the tricarboxylic acid (TCA) cycle and the mitochondrial electron transport chain (ETC), presumably to produce extra ATP for transporting malate into the vacuole for storage at night.

CAM idling

CAM idling is characterised by the lack of diel gaseous exchange and a small continued diel fluctuation in organic acids level because of internally recycled CO_2 (Sipes and Ting, 1985). It is usually an adaptation in water-stressed plants, which results in the closure of stomata for the whole day. To model this, the CO_2 and O_2 exchange during the day and night were constrained to carry zero flux. Given that there is no CO_2 exchange, we assumed that there is no net carbon fixation, hence phloem export was constrained to zero for CAM idling.

The primary metabolic demand for plants in CAM idling is cellular maintenance. The model predicted a starch-malate cycle where starch accumulated during the day is metabolised at night mainly through glycolysis and the oxidative pentose phosphate pathway (OPPP) to produce ATP and NADPH for maintenance processes. While the majority of PEP was used as precursor for carbon refixation by PEPC, a significant proportional of PEP was predicted to be metabolised further through the TCA cycle to feed the mitochondrial ETC for ATP synthesis. Given that it is a closed system with respect to carbon, CO_2 produced in the OPPP and the TCA cycle is refixed by PEPC which ultimately leads to the accumulation of malate in the dark. In the day, malate was predicted to be decarboxylated by primarily by PEPCK in our model. The resulting PEP is recycled to produce starch via gluconeogenesis, while the CO_2 produced from malate decarboxylation is refixed via the Calvin cycle similar to that in CAM. With no net carbon import or export, the amount of carbon stored in starch

during the day was predicted to be equalled to the amount of carbon storage in malate at night. The starch-malate cycle is primarily driven by the energy from the light reactions of photosynthesis, and it acts as a carbon neutral way of storing energy from the day to night.

Energetics and metabolite accumulation in C_3, CAM, CAM cycling and CAM idling

The metabolic flux predictions of C_3, CAM, CAM cycling and CAM idling were compared to see how CAM cycling and CAM idling fit into the evolution of CAM from C_3. Table 2 summarises the predicted fluxes related to energetics and metabolic accumulation in the four simulations. CAM idling was predicted to use the least amount of photon, which is expected given that it does not have the metabolic demand for exporting sucrose and amino acids into the phloem. For the same metabolic demand, CAM requires more photon than C_3 as expected. It is interesting to see that the photon demand for CAM cycling falls between C_3 and CAM. A similar trend was observed for other fluxes related to energy metabolism including the ATP and NADPH production by the photosynthetic light reaction and the ATP production by the mitochondrial ATP synthase (Table 2). The same trend was also reflected in the energetic demand in the Calvin cycle in terms of ATP and NADPH consumption (Supplemental Table S3).

Metabolite accumulation showed a different pattern compared to the energetics (Table 2). C_3 had the lowest daytime starch accumulation, followed by CAM cycling and CAM idling which had about 2-3 times more starch accumulation than C_3. CAM had the highest daytime starch accumulation with more than nine times the amount than C_3. This suggest that CAM cycling and CAM idling could potentially be an intermediate in CAM evolution with respect to the regulation of starch accumulation. A similar pattern can be observed for malate accumulation. A very small amount of malate was predicted to accumulate during the day for C_3 plants, whereas a large nocturnal malate accumulation was predicted for CAM as part of CAM photosynthesis. CAM cycling and CAM idling had intermediate level of nocturnal malate accumulation (~20% of that in CAM), which were related to the refixation of nocturnal CO_2 by PEPC. Reactions related to the starch-malate cycle, including glycolysis and PEPC at night and gluconeogenesis and PEPCK during the day, showed a similar trend (Supplemental Table S3) suggesting that CAM cycling and/or CAM idling could be an

evolutionary intermediate for the evolution of the extensive starch-malate cycle in CAM plants.

Predicting the metabolic transitions during C_3-CAM evolution

The behaviour of diel CO_2 exchange is the main diagnostic indicator between C_3 and CAM (Silvera et al., 2010). To model the potential metabolic transitions that could happen during the evolution of CAM from C_3, we varied the daytime CO_2 uptake from 13.12 μmol m^{-2} s^{-1} (the predicted value for C_3) to 0 μmol m^{-2} s^{-1} (which had the same effect as gradually increasing nocturnal CO_2 uptake given the overall carbon balance). This simulates the decrease in gaseous exchange during the day by stomata closure, hence a similar constraint was set for daytime oxygen exchange. As the stomata closes during the day, i.e. daytime CO_2 uptake decreases, it was assumed that the proportion of rubisco flux going through the carboxylase reaction increases linearly from 75% (carboxylase to oxygenase ratio of 3:1) to 83.74% (carboxylase to oxygenase ratio of 5.15:1) to account for the reduction of photorespiration. All other constraints remained the same as the C_3 and CAM simulations. This analysis simulates the closing of stomata which decreases CO_2 intake during the day. The results from this simulation can be found in Supplemental Table S4.

Given that the metabolic demands remained constant throughout the analysis, a decrease in daytime CO_2 uptake led to a shift from C_3 to CAM photosynthesis with an increase in flux through the starch-malate cycle including starch degradation, glycolysis, PEPC and malate accumulation at night, and malate decarboxylation via PEPCK and starch accumulation during the day (Figure 2a,b; Supplemental Table S4). Note that nocturnal CO_2 uptake increases as daytime CO_2 uptake decreases due to the carbon balance of the model in exporting a fixed amount of sucrose and amino acids into the phloem. CAM cycling occurs at the point when nocturnal CO_2 uptake is zero.

Despite the constrained decrease in rubisco oxygenase contribution as daytime CO_2 uptake decreases, the amount of energy (in terms of photon) required to sustain the same metabolic demand increases by about 7% from C_3 to CAM (Figure 2c) as extra energy is needed to run the starch-malate cycle. This is correlated with the increase in flux through the photosynthesis light reactions. Besides plastidial ATP synthesis, there was also an increase in ATP synthesis by the mitochondrial ETC in the day as the simulation shifted from C_3 to CAM (Figure 2d). The contribution of mitochondrial ATP synthesis increased from 18.2% in C_3 to 35.6% in CAM (Figure 2e), which is likely to be related to the increase in NADH produced during malate decarboxylation. In our simulations, the rubisco carboxylase flux was predicted to be remain relatively constant while the total rubisco flux (carboxylase +

oxygenase) decreases from C_3 to CAM due to the decrease in rubisco oxygenase activity (Figure 2f). There are two major factors affecting rubisco carboxylase flux, i) refixation of photorespiratory CO_2 and ii) starch accumulation to support energy demand at night. In this case, the two factors counteract each other throughout the simulation where photorespiration decreases and the energy demand for running the starch-malate cycle (mostly for pumping malate into the vacuole) increases from C_3 to CAM.

During the night, other than the increase in glycolytic flux as part of the starch-malate cycle from C_3 to CAM, the model predicted an 87% increase in flux through the TCA cycle and an 83% increase in flux through the mitochondrial ETC (Figure 2g). This increase in mitochondrial ATP synthesis was mostly used to support the ATP-dependent tonoplast proton pump for the increasing nocturnal vacuolar malate accumulation. The cytosolic OPPP flux was predicted to decrease by 30% in the night from C_3 to CAM (Figure 2h). This could be explained by the increase in the TCA cycle flux which contribute to the production of NADPH in the mitochondrion by the NADP-isocitrate dehydrogenase. This lessened the demand for the production of cytosolic NADPH required to be shuttled into the mitochondrion for maintenance processes.

Discussion

CAM cycling and CAM idling as viable evolutionary steps for establishing the starch-malate cycle

CAM cycling is considered as a weak form of CAM with stomata are open during the day and are closed at night (Lüttge, 2004; Silvera et al., 2010). With these constraints, our model predicted the known features of CAM cycling including the refixation of respiratory CO_2 at night and a small amount of nocturnal malate accumulation (Cushman, 2001). To support these metabolic behaviours, our model predicted the establishment of a starch-malate cycle in CAM cycling which includes increases in flux in malate decarboxylation, gluconeogenesis and starch synthesis and accumulation during the day and starch degradation and glycolysis at night compared to C_3 plants. The main metabolic advantage of CAM cycling over C_3 is its higher carbon conversion efficiency when photosynthesis is limited by daytime stomatal conductance, i.e. carbon limited. Given the same metabolic outputs, CAM cycling was predicted to require 20% less external CO_2 compared to C_3 due to the refixation

of nocturnal respiratory CO_2. This comes with a minor cost of 4.8% more photon and 1.6% more rubisco activity required assuming that there is no reduction in photorespiration, which could be affected by limiting stomatal conductance and internal CO_2 generation from malate decarboxylation. Given an environment that limits daytime stomatal conductance, e.g. high temperature and drought, the evolution of CAM cycling, together with the establishment of the starch-malate cycle, was predicted to be advantageous in maximising carbon conversion efficiency. The metabolic activities of all reactions in the starch-malate cycle in CAM cycling were predicted to be at an intermediate level between C_3 and CAM. The same applies to other supporting reactions such as the TCA cycle at night and the mitochondrial ETC during the day and night. These findings suggest that CAM cycling is likely to be a possible evolutionary step for the evolution of CAM photosynthesis.

As opposed to CAM cycling, CAM idling is thought of as a form of very strong CAM (Lüttge, 2004). In CAM idling, stomata remain closed throughout the day and night with small, sustained diel fluctuations in organic acids (Cushman, 2001; Silvera et al., 2010). By constraining our model with closed stomata during the day and night, the model predicted the operation of the starch-malate cycle as the most energy efficient way to sustain cellular activities. From an evolutionary perspective, if a plant often experiences conditions that require the closure of stomata throughout day and night, such as experiences long periods of severe drought, the evolution of CAM idling would be advantageous for the plant to stay alive. While the evolution of CAM through CAM cycling seems more likely given its similarities to C3, it is not impossible that some lineages could establish the starch-malate cycle through CAM idling.

Stomatal conductance as a determinant along the C_3-CAM continuum

It is currently accepted that CAM evolution is along a continuum from C_3 to CAM (Silvera et al., 2010; Bräutigam et al., 2017). Our model analysis showed that by varying the daytime CO_2 exchange, as a proxy for stomatal conductance, there exists a C_3-CAM continuum with gradual metabolic changes along the continuum (Figure 2). The key metabolic changes include the processes in the starch-malate cycle, the TCA cycle at night, and the chloroplastic and mitochondrial ETCs. The fact that a gradual continuum was predicted to be the most energetically favourable way to adapt to a change in stomata conductance suggests that the fitness landscape between C_3 and CAM is a smooth one. Given

our results, it is not surprising to see many facultative CAM plants which can easily switch between C_3 and CAM. Based on our model predictions, it is hypothesised that we could find plants anywhere on the C_3-CAM continuum. A prime example is CAM cycling which falls within the C_3-CAM continuum at the point when nocturnal CO_2 exchange is zero. Given the flexibility shown in facultative CAM plants and our results on the C_3-CAM continuum, it could be possible to find existing plants or engineer new plants that can switch not only between C_3 and CAM but also at different points on the continuum depending on the environmental conditions.

Conclusion

Using a core metabolic model of Arabidopsis, we were able to model the metabolic behaviours of CAM, CAM cycling and CAM idling by changing a few simple constraints on gaseous exchange and phloem export. Our results showed that CAM cycling and CAM idling could potentially be evolutionary intermediates in CAM evolution by establishing an intermediate flux through the starch-malate cycle. By varying the stomatal conductance, the model predicted a continuum from C_3 to CAM with gradual metabolic changes. Besides the insights gained in CAM evolution, the results from this study is informative to guide engineering efforts in introducing CAM into C_3 crops by identifying the metabolic changes required to convert C_3 to CAM. In additional to the starch-malate cycle involved in CAM photosynthesis, our model showed that the fluxes of other metabolic processes including the TCA cycle and the mitochondrial ETC need to be altered from C_3 to optimise CAM photosynthesis.

Materials and Methods

Core metabolic model for modelling C_3, CAM, CAM cycling and CAM idling

The mass- and charge-balance core metabolic model of Arabidopsis in Shameer et al. (2018) was used for modelling the metabolism of leaves operating in C_3, CAM, CAM cycling and CAM idling. A number of minor modifications were made to the Shameer et al. (2018) model. Firstly, an oxygen accumulation reaction was added to the model such that we could run the simulations for CAM and CAM idling as oxygen exchange was constrained to zero during the day in these two scenarios. Another modification from Shameer et al. (2018) was how the acidification of the vacuole was modelled. Instead of directly setting different fixed pH for the vacuole in C_3 and CAM, proton was allowed to accumulate in the vacuole in our model. A reaction allowing protons to freely flow in and out of the cytosol was blocked such that pH homeostasis can be modelled through the accumulation of protons in the vacuole. For linking the cytosolic and mitochondrial proton pools, proton transport between the cytosol and the mitochondrial intermembrane space was set to be reversible. The modification of this constraint only led to a very minor change in the flux predictions (data not shown). Irreversible proton transporters were added from the vacuole to the cytosol and from extracellular to the cytosol to allow leakage of protons down the electrochemical gradients. Lastly, the compartmentation of metabolites in the reaction "HEXOKINASE_RXN_MANNOSE_c" was corrected to be in the cytosol. The modified core model can be found in SBML and Excel formats (Supplemental File S1).

Model simulations with flux balance analysis

Based on the constraints and objective function stated in the Results section, parsimonious flux balance analysis (pFBA) was performed using scobra (https://github.com/mauriceccy/scobra), an extension of cobrapy (Ebrahim et al., 2013). The scripts for running the simulations in this study can be found in Supplemental File S2. The results from the individual pFBA simulations of C_3, CAM, CAM cycling and CAM idling (Supplemental Table S1) were verified using flux variability analysis (Mahadevan and Schilling, 2003; Supplemental Table S2).

Acknowledgements

We thank Yale-NUS College (WBS R-607-265-233-121) for the financial support.

Tables

Table 1: Sets of constraints for modelling C_3, CAM, CAM cycling and CAM idling. Phloem export rate was set based on the predicted value of C_3 plants in Shameer et al. (2018). Rubisco carboxylase:oxygenase ratio was set to 3:1 when stomata is opened, and 5.15:1 when stomata is closed based on Shameer et al. (2018).

Constraints ($\mu mol\ m^{-2}\ s^{-1}$)	**C_3**	**CAM**	**CAM Cycling**	**CAM Idling**
Phloem export	0.259	0.259	0.259	0
CO_2 exchange (day)	Unconstrained	0	Unconstrained	0
CO_2 exchange (night)	Unconstrained	Unconstrained	0	0
O_2 exchange (day)	Unconstrained	0	Unconstrained	0
O_2 exchange (night)	Unconstrained	Unconstrained	0	0
Rubisco carboxylase:oxygenase ratio (day)	3:1	5.15:1	3:1	5.15:1
Rubisco carboxylase:oxygenase ratio (night)	3:1	3:1	5.15:1	5.15:1

Table 2. Fluxes related to energetics and metabolic accumulation predicted in the model simulations of C_3, CAM cycling, CAM idling and CAM. Photon demand and ATP and NADPH production by photosynthetic light reaction happen during the day. A positive value of metabolite accumulation denotes a net accumulation in the day; negative value of metabolite accumulation denotes a net accumulation in the night. All values are in the units of μmol m^{-2} s^{-1}.

	C_3	CAM	CAM cycling	CAM idling
Photon demand	199.40	213.39	209.04	57.484
ATP production by photosynthetic light reaction	64.09	68.59	67.19	18.48
NADPH production by photosynthetic light reaction	46.80	51.38	49.15	14.06
ATP production by the mitochondrial ETC (day)	14.49	37.86	19.66	11.57
ATP production by the mitochondrial ETC (night)	7.20	13.20	8.39	8.27
Starch accumulation	0.86	8.14	2.35	1.94
Malate accumulation	0.04	-14.13	-2.84	-2.92

Figure Legends

Figure 1. Core sets of metabolic fluxes in the four modes of photosynthesis modelled: (A) C_3, (B) CAM, (C) CAM cycling and (D) CAM idling. The width of the arrows represents the magnitude of the reaction flux according to the scale on the bottom of the figure in μmol m^{-2} s^{-1}. The photorespiratory pathway is shown in chloroplast for simplicity, which in reality spans multiple compartments. Flux from 3-phosphoglycerate to PEP was taken as flux for glycolysis and gluconeogenesis. Flux for succinate dehydrogenase was taken as the TCA cycle flux. Rubisco carboxylase flux was taken as the flux through the Calvin cycle.

Figure 2. Model predictions of metabolic changes along the C_3-CAM continuum, as modelled by daytime CO_2 exchange, in (A) starch and malate accumulation, (B) nocturnal PEPC and daytime PEPCK fluxes, (C) photon intake, (D) daytime ATP synthesis plastidial and mitochondrial ATP synthases, (E) the proportion of daytime ATP synthesis by the mitochondrial ATP synthase, (F) rubisco carboxylase and oxygenase fluxes, (G) fluxes through the TCA cycle (taken as the flux of succinate dehydrogenase) and the mitochondrial ETC (taken as the flux of NADH dehydrogenase), and (H) nocturnal OPPP flux (taken as the sum of fluxes of plastidial and cytosolic glucose 6-phosphate dehydrogenases).

References

Borland, A.M., Hartwell, J., Weston, D.J., Schlauch, K.A., Tschaplinski, T.J., Tuskan, G.A., Yang, X., and Cushman, J.C. (2014). Engineering crassulacean acid metabolism to improve water-use efficiency. Trends in Plant Science *19*, 327–338.

Bräutigam, A., Schlüter, U., Eisenhut, M., and Gowik, U. (2017). On the Evolutionary Origin of CAM Photosynthesis. Plant Physiology *174*, 473–477.

Cheung, C.Y.M., Poolman, M.G., Fell, D.A., Ratcliffe, R.G., and Sweetlove, L.J. (2014). A Diel Flux Balance Model Captures Interactions between Light and Dark Metabolism during Day-Night Cycles in C_3 and Crassulacean Acid Metabolism Leaves. Plant Physiology *165*, 917–929.

Cushman, J.C. (2001). Crassulacean Acid Metabolism. A Plastic Photosynthetic Adaptation to Arid Environments. Plant Physiology *127*, 1439–1448.

Ebrahim, A., Lerman, J.A., Palsson, B.O., and Hyduke, D.R. (2013). COBRApy: COnstraints-Based Reconstruction and Analysis for Python. BMC Systems Biology *7*, 74.

Lüttge, U. (2004). Ecophysiology of Crassulacean Acid Metabolism (CAM). Annals of Botany *93*, 629–652.

Mahadevan, R., & Schilling, C.H. (2003). The effects of alternate optimal solutions in constraint-based genome-scale metabolic models. Metabolic engineering, *5*, 264-276.

Shameer, S., Baghalian, K., Cheung, C.Y.M., Ratcliffe, R.G., and Sweetlove, L.J. (2018). Computational analysis of the productivity potential of CAM. Nature Plants *4*, 165–171.

Silvera, K., Neubig, K.M., Whitten, W.M., Williams, N.H., Winter, K., and Cushman, J.C. (2010). Evolution along the crassulacean acid metabolism continuum. Functional Plant Biology *37*, 995.

Sipes, D.L., and Ting, I.P. (1985). Crassulacean Acid Metabolism and Crassulacean Acid Metabolism Modiffications in Peperomia camptotricha'. *77*, 5.

Ting, I.P. (1985). Crassulacean Acid Metabolism. Annu. Rev. Plant. Physiol. *36*, 595–622.

Winter, K., & Smith, J. A. C. (1996). An introduction to crassulacean acid metabolism. Biochemical principles and ecological diversity. In *Crassulacean acid metabolism* (pp. 1-13). Springer, Berlin, Heidelberg.

List of Supplemental Data

Supplemental Table S1: Flux solutions from parsimonious flux balance analysis for C_3, CAM, CAM cycling and CAM idling

Supplemental Table S2: Flux ranges from flux variability analysis for C_3, CAM, CAM cycling and CAM idling

Supplemental Table S3: A summary of predicted fluxes of key reactions in central metabolism from parsimonious flux balance analysis for C3, CAM, CAM cycling and CAM idling

Supplemental Table S4: Flux solutions from parsimonious flux balance analysis for the C_3-CAM continuum

Supplemental File S1: Core metabolic model for simulating C_3, CAM, CAM cycling and CAM idling in SBML and Excel formats

Supplemental File S2: Python scripts for running model simulations

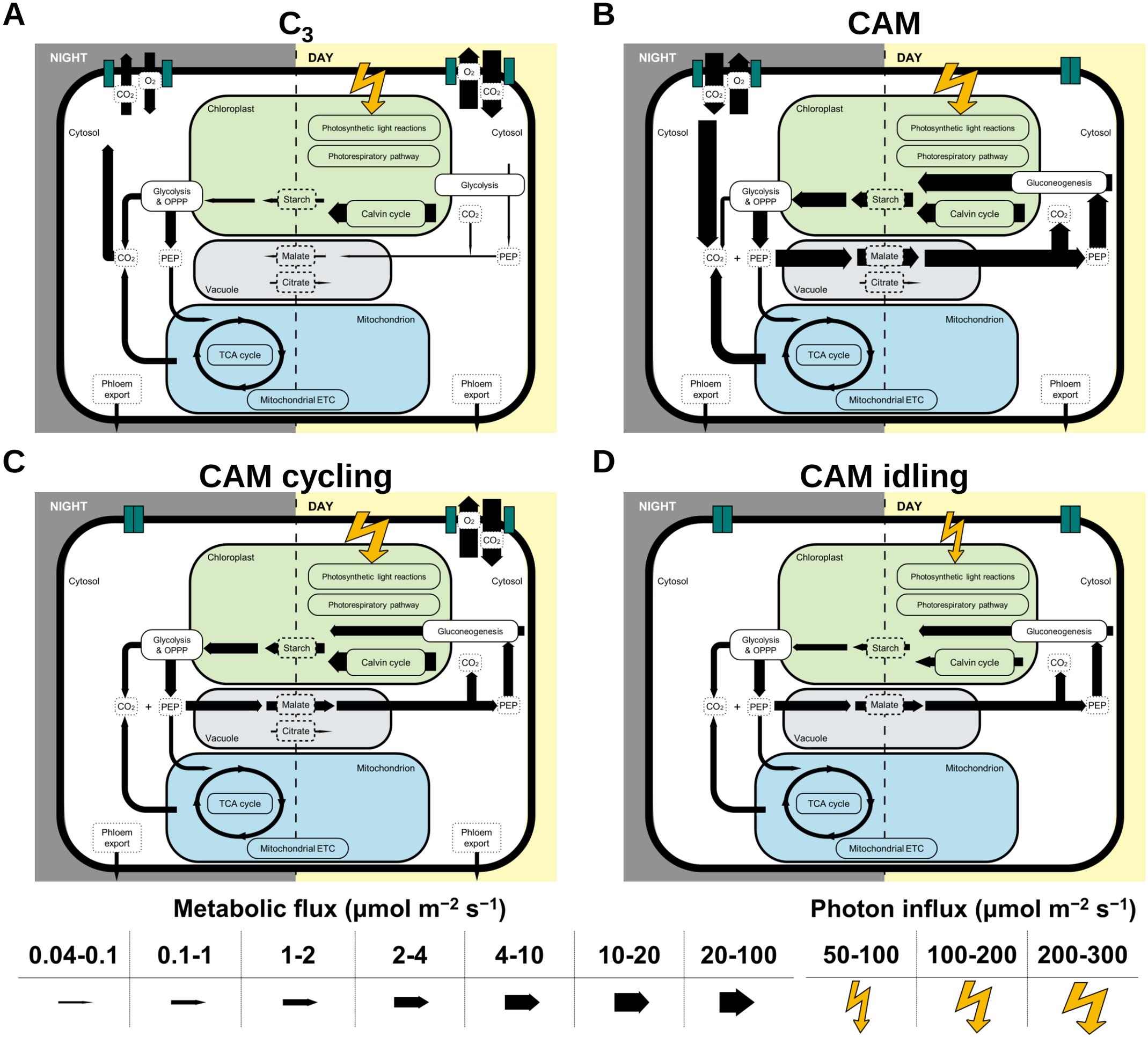
A
C3
NIGHT
DAY
O2
CO2
Chloroplast
Photosynthetic light reactions
Photorespiratory pathway
Cytosol
Glycolysis & OPPP
Starch
Calvin cycle
Glycolysis
PEP
Malate
Citrate
Vacuole
Mitochondrion
TCA cycle
Mitochondrial ETC
Phloem export
B
CAM
Gluconeogenesis
C
CAM cycling
D
CAM idling
Metabolic flux (μmol m−2 s−1)
0.04-0.1
0.1-1
1-2
2-4
4-10
10-20
20-100
Photon influx (μmol m−2 s−1)
50-100
100-200
200-300

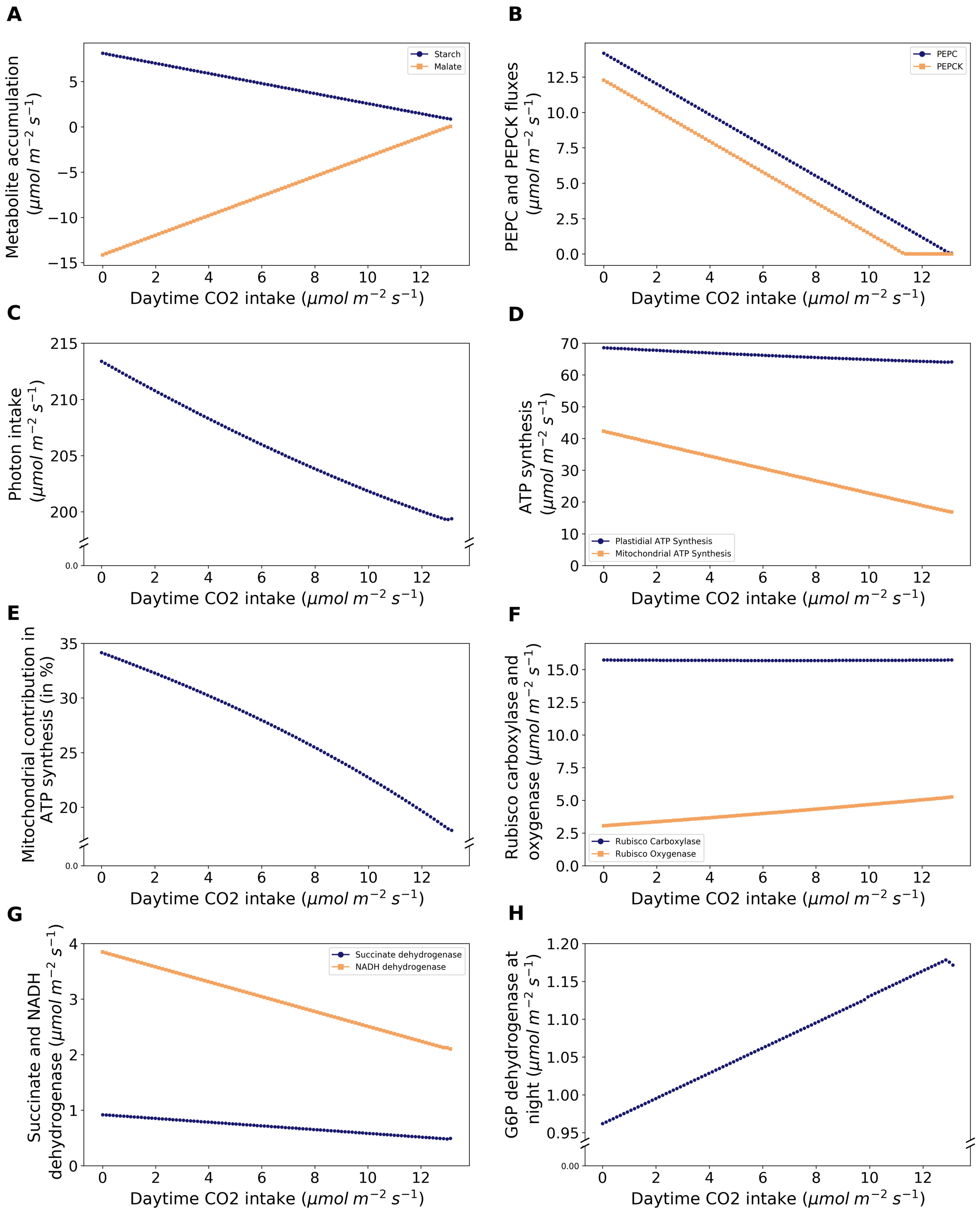
A
Metabolite accumulation ($\mu mol\ m^{-2}\ s^{-1}$)
Starch
Malate
Daytime CO2 intake ($\mu mol\ m^{-2}\ s^{-1}$)
B
PEPC and PEPCK fluxes ($\mu mol\ m^{-2}\ s^{-1}$)
PEPC
PEPCK
Daytime CO2 intake ($\mu mol\ m^{-2}\ s^{-1}$)
C
Photon intake ($\mu mol\ m^{-2}\ s^{-1}$)
Daytime CO2 intake ($\mu mol\ m^{-2}\ s^{-1}$)
D
ATP synthesis ($\mu mol\ m^{-2}\ s^{-1}$)
Plastidial ATP Synthesis
Mitochondrial ATP Synthesis
Daytime CO2 intake ($\mu mol\ m^{-2}\ s^{-1}$)
E
Mitochondrial contribution in ATP synthesis (in %)
Daytime CO2 intake ($\mu mol\ m^{-2}\ s^{-1}$)
F
Rubisco carboxylase and oxygenase ($\mu mol\ m^{-2}\ s^{-1}$)
Rubisco Carboxylase
Rubisco Oxygenase
Daytime CO2 intake ($\mu mol\ m^{-2}\ s^{-1}$)
G
Succinate and NADH dehydrogenase ($\mu mol\ m^{-2}\ s^{-1}$)
Succinate dehydrogenase
NADH dehydrogenase
Daytime CO2 intake ($\mu mol\ m^{-2}\ s^{-1}$)
H
G6P dehydrogenase at night ($\mu mol\ m^{-2}\ s^{-1}$)
Daytime CO2 intake ($\mu mol\ m^{-2}\ s^{-1}$)

Parsed Citations

Borland, A.M., Hartwell, J., Weston, D.J., Schlauch, K.A., Tschaplinski, T.J., Tuskan, G.A., Yang, X., and Cushman, J.C. (2014). Engineering crassulacean acid metabolism to improve water-use efficiency. Trends in Plant Science 19, 327–338.
Pubmed: Author and Title
Google Scholar: Author Only Title Only Author and Title

Bräutigam, A., Schlüter, U., Eisenhut, M., and Gowik, U. (2017). On the Evolutionary Origin of CAM Photosynthesis. Plant Physiology 174, 473–477.
Pubmed: Author and Title
Google Scholar: Author Only Title Only Author and Title

Cheung, C.Y.M., Poolman, M.G., Fell, D.A., Ratcliffe, R.G., and Sweetlove, L.J. (2014). A Diel Flux Balance Model Captures Interactions between Light and Dark Metabolism during Day-Night Cycles in C3 and Crassulacean Acid Metabolism Leaves. Plant Physiology 165, 917–929.
Pubmed: Author and Title
Google Scholar: Author Only Title Only Author and Title

Cushman, J.C. (2001). Crassulacean Acid Metabolism. A Plastic Photosynthetic Adaptation to Arid Environments. Plant Physiology 127, 1439–1448.
Pubmed: Author and Title
Google Scholar: Author Only Title Only Author and Title

Ebrahim, A., Lerman, J.A., Palsson, B.O., and Hyduke, D.R. (2013). COBRApy: COnstraints-Based Reconstruction and Analysis for Python. BMC Systems Biology 7, 74.
Pubmed: Author and Title
Google Scholar: Author Only Title Only Author and Title

Lüttge, U. (2004). Ecophysiology of Crassulacean Acid Metabolism (CAM). Annals of Botany 93, 629–652.
Pubmed: Author and Title
Google Scholar: Author Only Title Only Author and Title

Mahadevan, R., & Schilling, C.H. (2003). The effects of alternate optimal solutions in constraint-based genome-scale metabolic models. Metabolic engineering, 5, 264-276.
Pubmed: Author and Title
Google Scholar: Author Only Title Only Author and Title

Shameer, S., Baghalian, K., Cheung, C.Y.M., Ratcliffe, R.G., and Sweetlove, L.J. (2018). Computational analysis of the productivity potential of CAM. Nature Plants 4, 165–171.
Pubmed: Author and Title
Google Scholar: Author Only Title Only Author and Title

Silvera, K., Neubig, K.M., Whitten, W.M., Williams, N.H., Winter, K., and Cushman, J.C. (2010). Evolution along the crassulacean acid metabolism continuum. Functional Plant Biology 37, 995.
Pubmed: Author and Title
Google Scholar: Author Only Title Only Author and Title

Sipes, D.L., and Ting, I.P. (1985). Crassulacean Acid Metabolism and Crassulacean Acid Metabolism Modiffications in Peperomia camptotricha'. 77, 5.
Pubmed: Author and Title
Google Scholar: Author Only Title Only Author and Title

Ting, I.P. (1985). Crassulacean Acid Metabolism. Annu. Rev. Plant. Physiol. 36, 595–622.
Pubmed: Author and Title
Google Scholar: Author Only Title Only Author and Title

Winter, K., & Smith, J. A. C. (1996). An introduction to crassulacean acid metabolism. Biochemical principles and ecological diversity. In Crassulacean acid metabolism (pp. 1-13). Springer, Berlin, Heidelberg.
Pubmed: Author and Title
Google Scholar: Author Only Title Only Author and Title

List of Supplemental Data